MRI of Peliosis Hepatis: A Case Series Presentation With a 2022 Systematic Literature Update

Linda Calistri, MD, PhD,[1] Cosimo Nardi, MD, PhD,[1] Vieri Rastrelli, MD,[1]
Davide Maraghelli, MD,[1] Luigi Grazioli, MD,[2] Luca Messerini, MD,[3] and
Stefano Colagrande, MD[1]*

Background: Peliosis hepatis (PH) is a rare benign condition, characterized by hepatic sinusoidal dilatation and blood-filled cystic cavities, often found incidentally, with still challenging diagnosis by imaging due to polymorphic appearance.

Purpose: Based on a retrospective analysis of our series (12 patients) and systematic literature review (1990–2022), to organize data about PH and identify features to improve characterization.

Study Type: Retrospective case series and systematic review.

Population: Twelve patients (mean age 48 years, 55% female) with pathology-proven PH and 49 patients (mean age 52 years, 67% female) identified in 33 studies from the literature (1990–2022).

Field Strength/Sequence: 1,5-T; T1-weighted (T1W), T2-weighted (T2W), diffusion-weighted (DW), contrast-enhanced (CE) T1W imaging.

Assessment: We compared our series and literature data in terms of demographic (gender/age/ethnicity), clinical characteristics (symptoms/physical examination/liver test), associated conditions (malignancies/infectious/hematologic/genetic or chronic disorders/drugs or toxic exposure) percentage. On magnetic resonance imaging lesion numbers/shape/mean maximum diameter/location/mass effect/signal intensity were compared. PH pathological type/proposed imaging diagnosis/patient follow-up were also considered.

Statistical Tests: Joanna Briggs Institute (JBI) Critical Appraisal Checklist for Case Reports/Series quality assessment. Intraclass correlation and Cohen's kappa coefficients for levels of inter/intrareader agreement in our experience.

Results: Patients were mainly asymptomatic (92% vs. 70% in our study and literature) with associated conditions (83% vs. 80%). Lesions showed homogeneous T1W-hypointensity (58% vs. 65%) and T2W-hyperintensity (58% vs. 66%). Heterogeneous nonspecific (25% vs. 51%), centrifugal (34% vs. 8%), or rim-like centripetal (25% vs. 23%) patterns of enhancement were most frequent, with hypointensity on the hepatobiliary phase (HBP), without restricted diffusivity. Good inter- and intrareader agreement was observed in our experience. Concerning JBI Checklist, 19 out of 31 case reports met at least 7 out of 8 criteria, whereas 2 case series fulfilled 5 and 6 out of 10 items respectively.

Data Conclusion: A homogeneous, not well-demarcated T1W-hypointense and T2W-hyperintense mass, with heterogeneous nonspecific or rim-like centripetal or centrifugal pattern of enhancement, and hypointensity on HBP, may be helpful for PH diagnosis. Among associated conditions, malignancies and drug exposures were the most frequent.

Level of Evidence: 4

Technical Efficacy: Stage 2

J. MAGN. RESON. IMAGING 2023.

Peliosis hepatis (PH) is a rare benign condition that is characterized by sinusoidal dilatation associated with the formation of blood-filled cystic cavities in the parenchyma.[1] It was first reported by Wagner in 1861, and was later named "Peliosis" by Schoenlank in 1916, which stems from the Greek word "Pelios" that means "reddish" or "bluish," referring to the autopsy liver appearance in a young lady who died from miliary tuberculosis.[2,3] Epidemiological data are scarce, but hepatic involvement is the most frequent, occasionally occurring in any part of the reticuloendothelial system (i.e., bone marrow, spleen, or lymph-nodes); very few studies indicated that other organs such as parathyroid glands, lungs, and kidneys may be affected as well.[3–5] PH has been reported to be associated with several underlying debilitating conditions, such as hematologic malignancies, as well as medications, with a reported incidence of up to 22% in post-transplantation patients.[5,6] Histopathologically, it is classified into two types: parenchymal and phlebectic PH.[7] The first type consists of irregular spaces not lined by endothelium, while the second is characterized by regular spaces with endothelial lining.[7]

Regarding the clinical appearance, PH is frequently asymptomatic and thus often represents an incidental diagnosis.[8,9] It is a poorly known condition both to clinicians and radiologists, without pathognomonic imaging features and frequently misdiagnosed, being often confused with other benign and malignant lesions.[10–17] The vast majority of articles dealing with PH are case reports, and only very few manuscripts described its magnetic resonance imaging (MRI) features together with iconographic patterns.[8,18,19]

We have retrospectively analyzed 12 pathologically confirmed original MRI cases of PH, in addition to those identified following a systematic review of the literature, with the goal of identifying potential characteristic features of PH to enable its diagnosis by imaging.

Materials and Methods

This retrospective study was conducted in accordance with the Declaration of Helsinki (as revised in 2013). Patients' medical records and the Digital Imaging and Communications in Medicine (DICOM) files were anonymized before their extraction; the imaging reports were de-identified prior to the analysis. Therefore, patient care was not affected and patient privacy was maintained throughout. Institutional review board approved the retrospective analysis of the data while the written informed consent was waived based on the retrospective nature of this study.

Study Design

We conducted a multicenter retrospective case-based study by collecting MRI features, epidemiological and clinical data of patients diagnosed with PH between 2015 and 2022 from Careggi Hospital of Florence and Spedali Civili Hospital of Brescia Diagnostic Imaging Department. Additionally, we performed a systematic review of the literature from January 1990 to June 2022 gathering the full spectrum of MRI appearances as well as epidemiological and clinical data of PH, according to PRISMA guidelines (Preferred Reporting Items for Systematic Reviews and Meta-Analyses).[20]

Clinical Subjects

PATIENTS AND METHODS. The patient search and selection process used in the two aforementioned hospitals are reported (Fig. 1). Inclusion criteria were: studies involving MRI examinations with T1-/T2-weighted (T1W/T2W), contrast-enhanced T1W (CE-T1W), diffusion-weighted (DW) images and a pathology-proven diagnosis of PH. Incomplete studies, those with uninterpretable MRI examinations due to artifacts or reporting a diagnosis not histologically confirmed, were excluded.

By analyzing medical records, we obtained patient demographic data (gender, age, and ethnicity), clinical characteristics (symptoms, physical examination findings, or liver test function abnormalities), history of associated conditions (malignancies, infectious, hematologic, genetic or other chronic disorders, drugs or toxic exposure), and pathological type of PH (parenchymal or phlebectic). When available, follow-up examinations were analyzed. We obtained the proposed imaging diagnosis by reviewing the reports.

IMAGING PROTOCOLS. Acquisitions were performed with 1.5-T MRI body scanners (Aera and Avanto at Careggi Hospital of Florence and Spedali Civili Hospital of Brescia, respectively; Siemens Healthineers, Erlangen, Germany) with a maximum gradient strength of 45 mT/m, a peak slew rate of 200 mT/m/msec, and a 4-channel phased array body coil. The acquisition protocol was reported (Table 1).

The apparent diffusion coefficient (ADC) map was automatically calculated on a picture archiving and communication system (PACS) workstation. CE-MRI data were obtained after the administration of a dose of 0.025 mmol/kg of body weight of liver-specific CA (gadolinium ethoxybenzyl-diethylenetriaminepentaacetic acid, Gd-EOB-DTPA, Primovist; Bayer Schering, Berlin, Germany) followed by 20 mL of sterile saline solution, injected via the antecubital vein, with a flow rate of 1 mL/s using a power injector (Veris; Medrad Inc., Pittsburgh, PA, USA). A three-dimensional (3D) gradient-recalled echo T1W breath-hold sequence with fat suppression was acquired before and after the intravenous administration of Gd-EOB-DTPA. The delay for the hepatic artery phase was determined by Care Bolus technique (mean delay time, approximately 30 seconds); the acquisition was repeated again at 70, 180 seconds, and 20 minutes during the portal vein, transitional, and hepatobiliary phase (HBP), respectively.

IMAGE ANALYSIS. All examinations were evaluated by three independent radiologists, one with 30 years of experience (S.C.) and two radiologists with 15 years of experience (L.C. and C.N.) in abdominal imaging. The assessment was carried out twice by each reader, with an interval of 1 month, using a PACS workstation (version Syngo plaza-VB30D Siemens Medical Healthineers, Erlangen, Germany). Number of lesions, shape (round, oval, or irregular), boundaries (ill-defined or well demarcated), and mean maximum
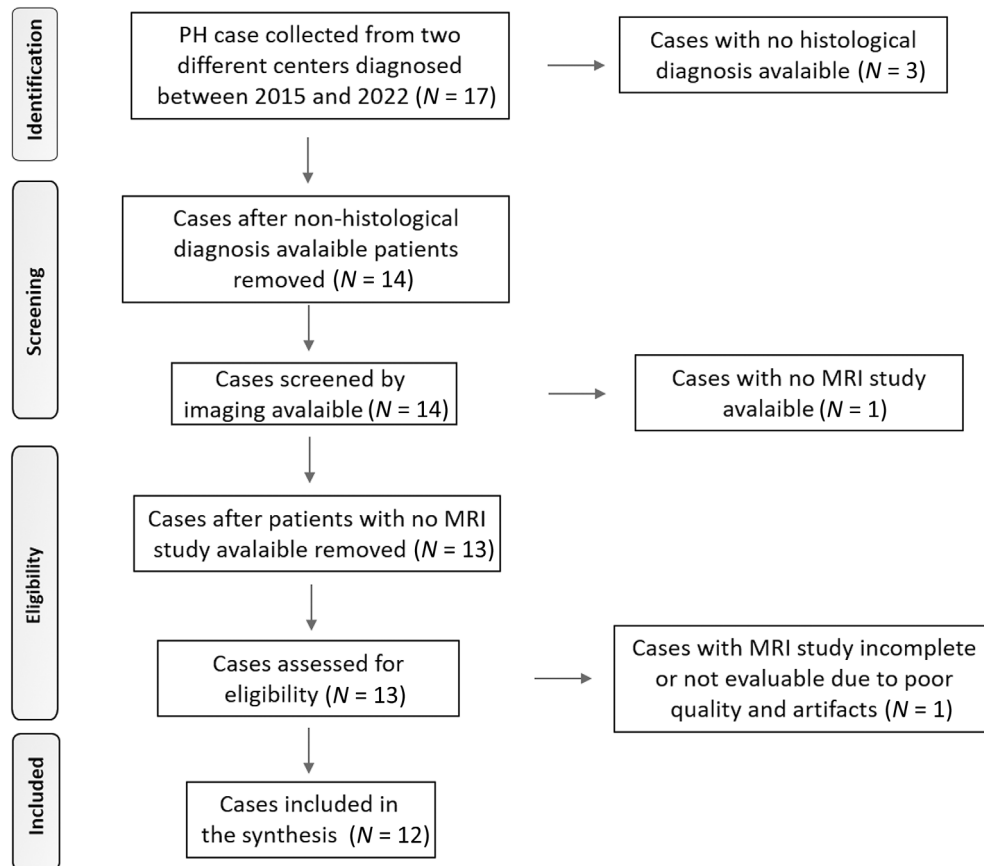
Identification

PH case collected from two different centers diagnosed between 2015 and 2022 (*N* = 17) → Cases with no histological diagnosis avalaible (*N* = 3)

Screening

Cases after non-histological diagnosis avalaible patients removed (*N* = 14)

Cases screened by imaging avalaible (*N* = 14) → Cases with no MRI study avalaible (*N* = 1)

Eligibility

Cases after patients with no MRI study avalaible removed (*N* = 13)

Cases assessed for eligibility (*N* = 13) → Cases with MRI study incomplete or not evaluable due to poor quality and artifacts (*N* = 1)

Included

Cases included in the synthesis (*N* = 12)

FIGURE 1: Flow diagram showing our patients search and selection process.

TABLE 1. MRI Protocol With Acquisition Parameters

	Axial GRE T1W In/Out Phase	Axial FS TSE T2W	Axial HASTE T2W	Coronal HASTE T2W	3D Axial FS GRE T1	Axial EPI SE DW 0–750 mm^2/s
TR, msec	170/490	1000/5254	327	1000/5294	3.26/4.4	6000
TE, msec	1.59/3.26	85/106	96	92/97.50	1.5/2	63
FOV, mm, AP-RL	300–420	300–420	390	300–420	300–420	420
Matrix	104 × 256	104 × 256	104 × 256	104 × 256	104 × 256	104 × 256
Thickness, mm	4–6	4–6	4–6	4–6	2.3–3	4–6
Fat sat method	Dixon	SPAIR	N/A	N/A	SPAIR	SPAIR

GRE = gradient-recalled echo; T1W = T1 weighted; FS = fat saturation; TSE = turbo spin echo; T2W = T2 weighted; HASTE = half-Fourier acquisition single-shot turbo spin echo; 3D = three-dimensional; EPI = echo planar imaging; SE = spin echo; DW = diffusion weighted; TR = repetition time; TE = echo time; FOV = field of view; AP = anterior–posterior; RL = right–left; SPAIR = spectral attenuated inversion recovery; NA = not applicable.

diameter were evaluated on the unenhanced T1W images, which ensured the best spatial and contrast resolution.

Regarding the lesion site, when PH extended to more than one segment, all segments were considered as affected. In accordance with Coinaud's liver subdivision scheme, segments 1–4 and 5–8 were considered as parts of the left and right lobe, respectively.[21] Percentages of segment involvement and lobe localization

were calculated, and mass effect was reported if lesion(s) caused displacement or compression on the biliary or blood vessels. The signal intensity (SI) of each lesion on T1W/T2W/CE-T1W/DW images and ADC map was visually assessed. SI was defined in comparison with the surrounding parenchyma, as follows: homogeneous hypo/iso/hyperintensity, if uniform; heterogeneous, if not homogeneous; in this case the lesion was defined according to

dominant SI (hypo/iso/hyper), and the lesser foci (ring/central core SIs) were described.

Based on CE-T1 dynamic imaging, each lesion's pattern of enhancement was described as: homogeneously high or persistently low in all dynamic phases; rim-like centripetal (with enhancement from the periphery to the center), or centrifugal (in the opposite direction); heterogeneous nonspecific in the remaining cases. The presence/absence of "target sign" aspect (globular central vessel-like enhancement) was evaluated. After assessing the inter- and intra-reader agreement, discrepancies were resolved by consensus between the three readers. The mean maximum diameter was derived from the mean of the measurements obtained by each observer. Possible associations between enhancement patterns, pathology, associated conditions, proposed diagnosis, and follow-up were investigated.

STATISTICAL ANALYSIS. Collected data were analyzed using the SPSS® v. 26.0 statistical analysis software (IBM Corp., New York, NY; formerly SPSS Inc., Chicago, IL).

Intra- and interreader agreements were determined for each designated parameter as follows:

- Cohen's kappa was calculated for categorical variables used to analyze lesion number, shape, boundaries and site, as well as SI on MR sequences, pattern of enhancement, target sign in arterial phase, and mass effect. Kappa values of 0.01–0.20, 0.21–0.40, 0.41–0.60, 0.61–0.80, 0.81–0.99, and 1 represented slight, fair, moderate, substantial, almost perfect, and perfect agreement, respectively.
- Intraclass correlation coefficient (ICC) was used for the only continuous variable represented by the mean maximum diameter. The ICC values of 0.00–0.10, 0.11–0.40, 0.41–0.60, 0.61–0.80, and 0.81–1.0 represented no, slight, fair, good, and very good agreement, respectively.

Literature Data

SEARCH STRATEGY. An online database search on PubMed (https://pubmed.ncbi.nlm.nih.gov), Scopus (https://www.scopus.com/home.uri), and Web of Science (https://www.webofscience.com/wos/woscc/basic-search) was performed selecting studies that were published between January 1, 1990, and July 30, 2022. Our systematic review was based on the following PICO questions[22]: does a systematic literature review (I) and new case series (P) provide the imaging elements needed to accurately distinguish peliosis (O) from many other hepatic focal lesions (C)? The keywords used for the literature search were ((peliosis[Title]) AND (hepat*[Title]) AND (imaging[Title])).

STUDY SELECTION. Search results were evaluated and selected on the basis of titles and abstracts; duplicates were excluded. Abstracts and full texts of all the studies that emerged from the search were matched against our study inclusion criteria. The selection of studies meeting the inclusion criteria was independently conducted by two reviewers (V.R. and D.M., 7 years of experience in abdominal imaging, respectively). In case of diverging opinions between reviewers on including a study, a final consensus was reached through the input of a third reviewer (S.C., 30 years of experience in abdominal imaging). The study search and selection process are reported (Fig. 2). The inclusion criteria were as follows: publications written in English with PDF available; presence of MRI information, including at least one of the following sequences: T1W/T2W, CE-T1W, and/or DW sequences; presence of at least one illustrative figure of PH (to exclude meta-analyses, reviews, or commentary without original case/s); and presence of epidemiological (at least age and sex) and clinical data (information about symptoms, or physical examination or liver test function) of patients with pathology-proven PH. References of the included studies were also evaluated.

QUALITY ASSESSMENT. Quality assessment of the selected articles was independently performed by two reviewers (V.R. and D.M.) who evaluated the entire literature database. Disagreements were resolved by the independent judgment of a third reviewer (S.C.). The overall quality of case reports and series was evaluated using the Joanna Briggs Institute (JBI) Critical Appraisal Checklist for Case Reports[23] and for Case Series,[24] respectively; these checklists include items about patient inclusion criteria, clinical and procedural management, outcome/follow-up information, and take-home messages.[23] Both scales aim to assess the methodological quality of a study and examine its characteristics with several items requiring answers schematized as "yes," "no," "unclear" or "NA" if the item was not applicable.[24]

DATA EXTRACTION. The full text of the selected studies was analyzed. Data extraction was performed filling a form designed to address the search questions consisting of: article title; patient demographics (gender, age, and ethnicity); clinical characteristics (symptoms, physical examination, or liver test function abnormalities); associated conditions (malignancies, infectious, hematologic, genetic or other chronic disorders, drugs or toxic exposure); number of lesions, shape, mean maximum diameter, location, and spatial relationship with biliary and blood vessels; SI on T1W/T2W/CE-T1W images, DW images and ADC map; proposed imaging diagnosis; pathological type of PH; and follow-up information. In a way similar to our case series, when literature PH sites extended to more than one segment, all segments were considered as affected. Similarly, percentages of lobe localization, in accordance with Coinaud's liver subdivision scheme[21] were calculated. Extracted data were collected in a Microsoft Excel spreadsheet (version 18.2210.1203.0; Microsoft Corp., Redmond, WA, USA). Data extraction was performed by the same two reviewers (V.R. and D.M.) independently by using a specific and standardized form. Disagreements were resolved by the independent input of a third reviewer (S.C.), which checked all extracted data.

Results

Patient Selection for Our Cases

Out of 17 cases collected retrospectively, 3 were excluded due to the absence of a histological diagnosis, and 2 due to incomplete MRI examinations, with 12 patients meeting our inclusion criteria (Fig. 1).
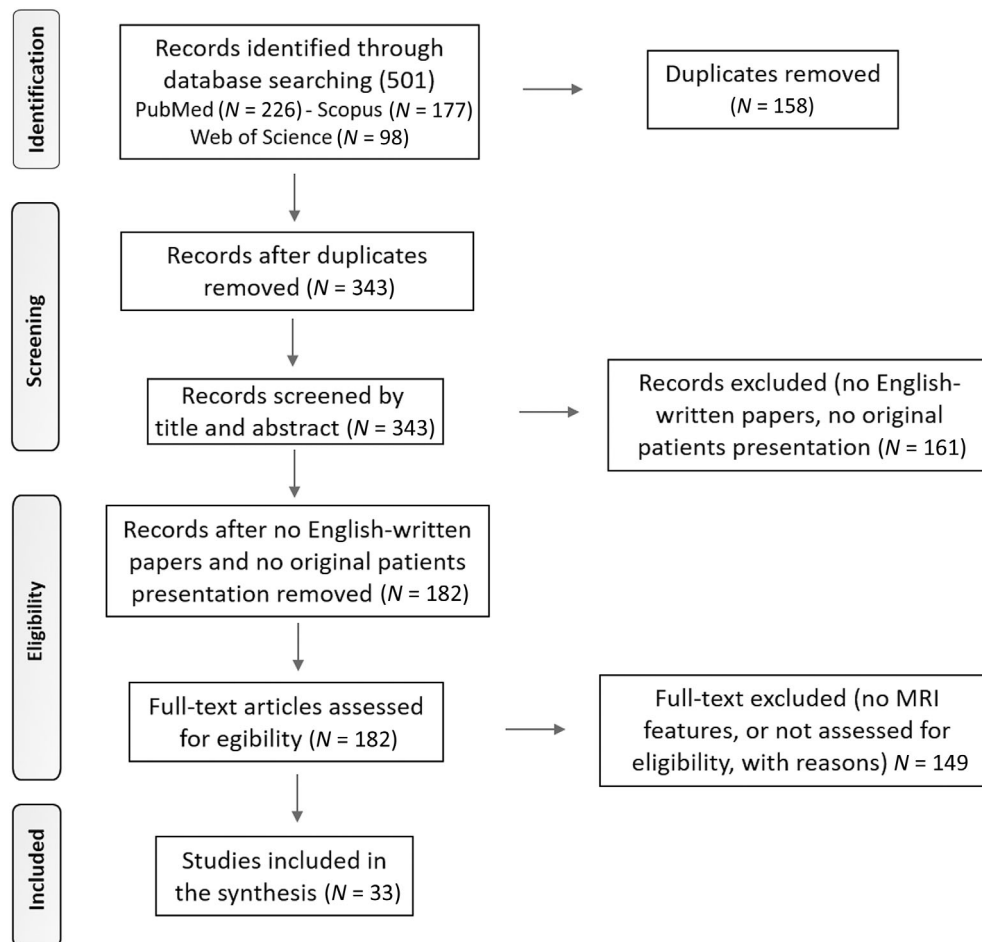
FIGURE 2: Flow diagram showing the study search and selection process.

Reader Agreements for Our Cases

As regard to the categorical variables, both intra- and interreader agreements were good, with kappa values ranging from 0.75 to 0.94 (substantial to almost perfect agreement).

Moreover, with regard to the mean maximum diameter, a very good agreement was found, both within each single reader (intrareader reliability) and between the three observers (interreader reliability), with ICC values ranging from 0.84 to 0.93 and from 0.82 to 0.90, respectively.

Literature Data

The initial search produced 501 studies. After selection, 33 articles were reviewed (Fig. 2): 2 case series/original articles[25,26] and 31 case reports,[2,3,5,6,10,11,17,27-50] for a total of 49 histologically confirmed PH patients (Fig. 2).

Regarding quality assessment, among the 31 case reports, 19 met at least 7 out of 8 criteria from the JBI Appraisal Checklist for Case Reports, considering that the parameter referring to adverse events/unanticipated events was deemed as not applicable in 18 out of 31 case reports.

The two case series fulfilled 5 and 6 out of 10 items from JBI Appraisal Checklist for Case Series respectively, as they did not clearly report inclusion criteria nor follow-up

data or clear clinical information. So, statistical analysis was not deemed useful. Quality assessment results are available (Supplemental Material 1). It should be underlined that the vast majority of these studies did not report the complete characteristics of the lesions in all MR sequences.

Epidemiological and Clinical Features

Clinical data derived from our series included four males (33%) and eight females (67%), with a mean age of 52 years (age range 36–84 years), all Caucasians (our main patient population). They were asymptomatic in 11 (92%) cases, but 1 patient presented recurrent abdominal pain. In five (42%) patients, the lesions were detected on follow-up exams. Ten (83%) patients had associated conditions (Table 2) at the time of PH detection, and the majority were patients on hormonal and antimetabolites/antineoplastic drugs (50%). In four (33%) patients, hepatomegaly was detected. Liver function tests were normal in all patients.

Out of 49 patients from the literature, 22 were male (45%) and 27 were female (55%), with a mean age of 48 years (age range 9–78 years), prevalently Asians (70%), likely due to a higher number of Asian papers included in the analysis. Symptoms were present in 30% of cases, and in

TABLE 2. Conditions Associated to Peliosis Hepatis

Malignancies	Infections	Hematologic Disorders	Drugs	Toxicity	Others
- *Hepatocellular carcinoma*	- *Tuberculosis*	- *Spherocytic hemolytic anemia*	- *Hormonal therapy*[2,10,27,39]: **oral contraceptives**[5,31,37], **4 Pts**, *anabolic steroids*[28,29,33], *danazol, diethylstilbestrol, megestrol acetate*[42]	- *Toxins: polyvinyl chloride, arsenic, thorium oxide, cadmium, urethane*	- *Cardiac, liver, renal transplantation*[6]
- *Seminoma*	- *Leprosy*	- *Aplastic anemia*	- *Corticosteroids*[6,32]	- *Chronic alcohol consumption*	- *Chronic renal failure*[49]
- *Hodgkin's lymphoma*	- *Sifilidis*	- *Idiopathic thrombocytopenic purpura*[2]	- *Antimetabolites and/or antineoplastic*[2,26,34]: *azathioprine 2-Chloro-3'-deoxyadenosine, methotrexate tamoxifen,*[32] *thiopurine, 6-thioguanine,* **cisplatin 2 Pts**, *oxaliplatin*[40] **capecitabine**[40, 1 Pt], **etoposide**[1 Pt], **durvalumab**[1 Pt]	- *Vitamin A toxicity*	- *Diabetes mellitus*
- *Leukemias*	- *Bartonella henselae; Bartonella quintana bacillus (in HIV and immunocompromised patients)*[35]	- *Myeloproliferative disease*	- *Contrast agent: lipiodol*	- **Cocaine abuse**[1 Pt]	- *Arteritis*
- *Prostate cancer*[39]	- *Pyelonephritis*	- *Castleman's disease*	- *Iron chelators*		- *Intestinal lymphangiectasia*
- *Colorectal cancer*[26(9 Pts),34,40]	- **Biliary tract infection**[43, 1 Pt]	- *Malignant histiocytosis*	- *Immunoglobulin therapy*		- *Portal hypertension*
- **Gastric cancer**[25(2 Pts),30, 1 Pt]	- *Bacterial endocarditis*	- *Multiple myeloma*	- *Immunosuppressive agents: 6-mercaptopurine, cyclosporine*[6]		- *Portal vein aneurysms*
- *Pancreatic cancer*	- *Hepatitis C virus*[25(2 Pts),41]	- *Waldenstrom macroglobulinemia*	- **Interferon-beta therapy**[1 Pt]		- *Celiac and Chron's disease*
- *Renal cell carcinoma*[49]	- *Hepatitis B virus*[25]	- *Agnogenic myeloid metaplasia*			- *Wasting disease*

TABLE 2. Continued

Malignancies	Infections	Hematologic Disorders	Drugs	Toxicity	Others
- **Lung cancer**[17,38] , **1 Pt**		- *Fanconi disease*[28,29,33]			- *Pregnancy*
- *Breast cancer*[32]					- *Rheumatic disease: rheumatoid arthritis, systemic lupus erythematosus, Sjogren's syndrome*
- *Endometrial cancer*[42]					- *Genetic disorder: hereditary hemorrhagic telangiectasia, cystic fibrosis, X-linked myotubular myopathy*
					- **Common variable immunodeficiency**[48], **1 Pt**

Pt, patient (bold fonts: our experience; italic fonts: literature, with superscripted reference). In our experience, 1 Pt with lung cancer was treated with cisplatin, etoposide, and durvalumab association; 1 Pt with gastric cancer with cisplatin and capecitabine association.

70% of the patients PH was an incidental finding. The most frequent symptom was upper abdominal pain (20% of cases), followed by fever (6%), weight loss (6%), and fatigue (6%). On physical examination, hepatomegaly was present in 12% of patients. A nonspecific increase in liver function tests was observed in 12% of patients. In 18 (37%) patients, the lesions were new with respect to previous imaging exams.

Associated conditions were present in 39 (80%) patients, as shown in Table 2. The most frequent associated conditions were treatment with hormonal and antimetabolites/antineoplastic drugs (35% of patients), and colorectal and gastric cancer among the malignancies (29%).

Lesion Location and Their Relationship With Biliary and Blood Vessels

In our experience, five (42%) patients had only one lesion. The others had multiple lesions (17% between 2 and 5 lesions, 17% between 6 and 10, and 24% more than 10 lesions).

Lesions were located in the right lobe, the left lobe, or both in 33%, 17%, and 50% of the patients, respectively, without a preferential segment site. The mean maximum diameter of measurable PH nodules was 27 mm (size range 3–63 mm). One patient had confluent, unmeasurable lesions in the right lobe (Fig. 3). A round or oval-shaped lesion was found in 50% of cases, while irregular shapes were found in the other half of patients. Ill-defined and well-demarcated boundaries were shown in 43% and 57% of cases, respectively.

After reviewing the literature, 27 (56%) patients had single/isolated lesions with the remaining 22 (44%) presenting multiple lesions (16% between 2 and 5 lesions; 8% between 6 and 10 lesions; 20% more than 10 lesions).

Lesions were located in the right lobe, the left lobe, or both in 56%, 11%, and 33% of the patients, respectively, without a preferential segment site. Fifty-four percent of patients had PH nodules less than 20 mm, 38% between 21 and 50 mm, 8% greater than 50 mm, with a mean maximum diameter of 23.5 mm (size range 6–130 mm). The shape of the lesion was round/oval in 74% of patients and irregular in 26%. Ill-defined and well-demarcated boundaries were described in 55% and 45% of patients, respectively. Mass effects on vascular and biliary vessels were not observed neither in the literature nor in our experience.

Lesion Signal Intensity on Unenhanced MRI

All possible imaging patterns found on unenhanced images, together with the relative percentages of presentation, are summarized (Table 3). Patients of our series showed homogeneous (58%) or heterogeneous hypointensity (42%) on T1W images, the latter including lesions with isointense foci (25%) and "targetoid" lesions with hyperintense ring (17%). On T2W imaging, 58% of patients had homogenous hyperintense lesions, and 42% had heterogeneous lesions with isointense foci. Heterogeneous lesions on T1W images maintained a heterogeneous appearance on T2W imaging in all cases. On images with high b-values (750 mm^2/s) from DW acquisitions, 83% of patients had lesions showing signal hyperintensity, with ADC values equivalent to (25%) or higher than (50%) that of the surrounding parenchyma. A targetoid appearance with peripheral hyperintense halos and hypointense core was observed in two patients (17%), both on DW images and ADC maps (Fig. 4).

Most of the lesions described in the literature showed homogeneous T1W-hypointensity (65% of patients) and homogeneous T2W-hyperintensity (66%), and, on images
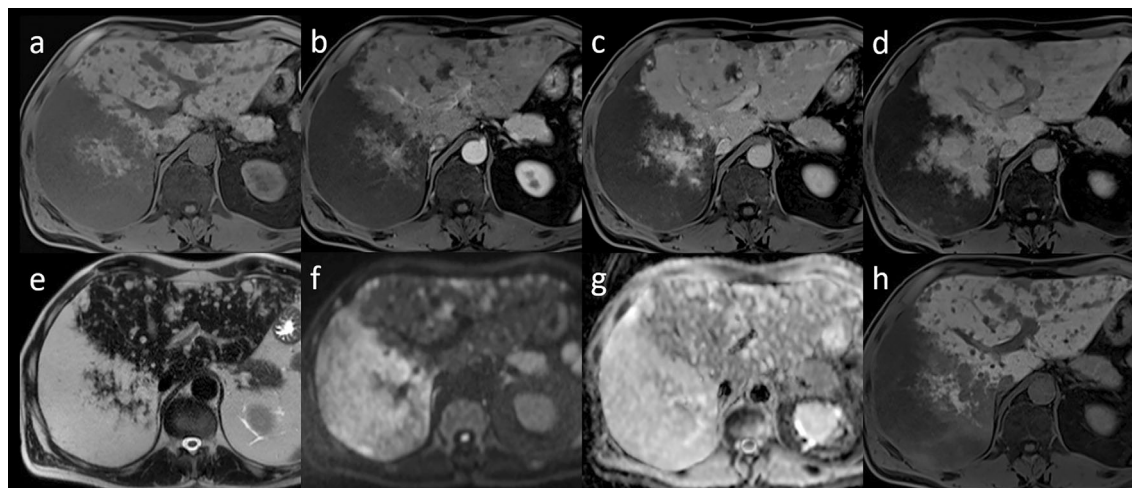

FIGURE 3: A 67-year-old male with histologically proven idiopathic diffuse peliosis without associated conditions. On MRI multiple lesions are observed in both hepatic lobes. The largest lesions are confluent in the right lobe, showing hypointensity on unenhanced T1-weighted images (a), centrifugal enhancement from arterial (b) to portal (c) and transitional (d) phase, hyperintensity on T2-weighted (e) images. On high b-value DWI (f) and ADC map (g) no signs of restricted diffusion are visible. Hypointensity on hepatobiliary phase (h) is shown.

TABLE 3. Imaging Patterns Found on Unenhanced T1-Weighted, T2-Weighted, Diffusion-Weighted Images and Apparent Diffusion Coefficient Map, and the Relative Percentages of Presentation

	T1				T2				DWI b-Value 750 mm²/s			ADC Map			
	Hypo-intensity	Hyper-intensity	Iso-intensity	Heterogeneous	Hypo-intensity	Hyper-intensity	Iso-intensity	Heterogeneous	Iso-intensity	Hyper-intensity	Heterogeneous	Hypo-intensity	Hyper-intensity	Iso-intensity	Heterogeneous
n	*n: 37*	*n: 37*	*n: 37*	*n: 37*	*n: 41*	*n: 41*	*n: 41*	*n: 41*	*n: 7*	*n: 7*	*n: 7*	*n: 0*	*n: 0*	*n: 0*	*n: 0*
Literature	*24/37*	*4/37*	*1/37*	*8/37*	*0/41*	*27/41*	*3/41*	*11/41*	*4/7*	*3/7*	*0/7*	*-*	*-*	*-*	*-*
%	*(65%)*	*(11%)*	*(2%)*	*(22%)*	*(0%)*	*(66%)*	*(7%)*	*(27%)*	*(57%)*	*(43%)*	*(0 %)*	*-*	*-*	*-*	*-*
n	**n: 12**	**n: 12**	**n: 12**	**n: 12**	**n: 12**	**n: 12**	**n: 12**	**n: 12**	**n: 12**	**n: 12**	**n: 12**	**n: 12**	**n: 12**	**n: 12**	**n: 12**
Our cases	**7/12**	**0/12**	**0/12**	**5/12**	**0/12**	**7/12**	**0/12**	**5/12**	**0/12**	**10/12**	**2/12**	**1/12**	**6/12**	**3/12**	**2/12**
%	**(58%)**			**(42%)**		**(58%)**		**(42%)**		**(83%)**	**(17%)**	**(8%)**	**(50%)**	**(25%)**	**(17%)**

N = number of patients for whom the data are available. Bold fonts: our experience. Italic fonts: literature. Literature data references: T1[2,3,5,6,10,11,17,25(3 pts),26(9 pts),27-31,32(2 pts),33-44,46-49]; T2[2,3,5,6,10,11,25(3 pts),26(9 pts),27-31,32(2 pts),33-36,38-40,44-47,49]; DWI[35,36,38,40-42,46].
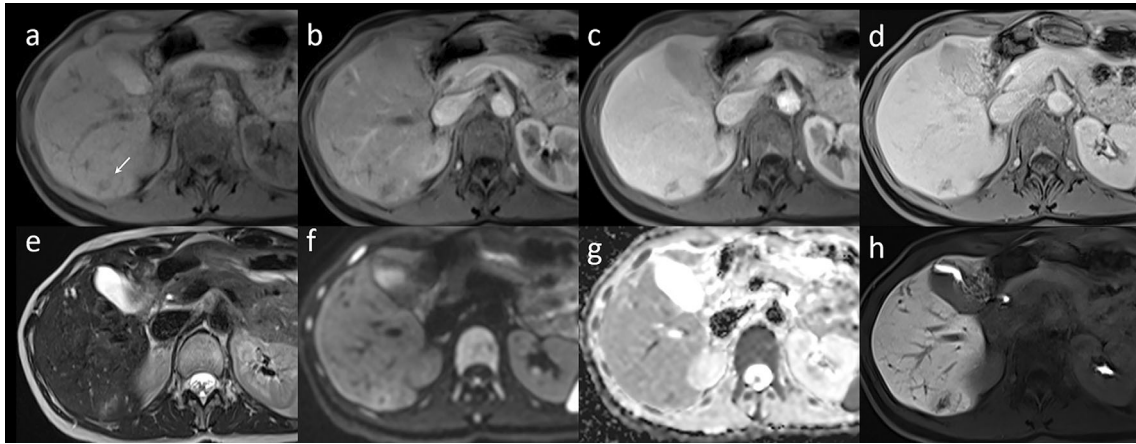DWI = diffusion-weighted imaging; ADC = apparent diffusion coefficient.

FIGURE 4: A 41-year-old female taking oral contraceptives for 2 years. During MRI follow-up for hepatic hemangioma (not shown), a new onset nodule is observed in segment 6. It shows iso-hypointensity on unenhanced T1-weighted image (a, white arrow), heterogeneous nonspecific pattern of enhancement on arterial (b), portal (c) and transitional (d) phase, heterogeneous hyperintensity on T2-weighted image (e). Targetoid appearance with peripheral hyperintense halos and hypointense core was observed both on high b-value DWI (f) and on ADC map (g). Heterogeneous hypointensity with foci of relative hyperintensity is shown on hepatobiliary phase (h). On histological examination dilated sinusoids with regressive changes in the surrounding parenchyma suggestive for PH were detected.

with high b-values (750 mm^2/s) from DW acquisitions, homogeneous isointensity (57%), or hyperintensity (43%). The literature did not report ADC values.

T1W-heterogeneous lesions (22% of patients) included hypointense lesions with iso- (10%) or hyperintense (6%) foci, and with "targetoid" appearance with hyperintense central core (6%). Furthermore, T2W-heterogeneous lesions (27% of patients) included hyperintense lesions with iso-intense foci (23%) and with "targetoid" appearance (4%, with hypointense central core). The T1W-heterogeneous lesions appeared heterogeneous on T2W images in 75% of cases. Multiple PH nodules in the same liver showed similar imaging features, except for three patients, presenting with more than 10 lesions, where only larger lesions showed heterogeneous T1W and T2W SI.

Patterns of Enhancement

In our study, Gd-EOB-DTPA was used in all cases (Table 4). The lesions mainly showed centrifugal (34% of patients) (Fig. 5), heterogeneous nonspecific (25%), and rim-like centripetal (25%) enhancement (Fig. 6). Considering single phases, the following observations have been made: on arterial phase, 42% of patients showed a peripheral rim enhancement, 33% hyperintensity (homogeneous or heterogeneous with small foci relatively less hyperintense), 17% target sign aspect; on transitional phase, 92% of patients showed homogeneous iso- to hyperintensity or heterogeneous hyperintensity with foci relatively less hyperintense; on HBP, all patients showed hypointense lesions. A schematic representation of the most common pattern of contrast enhancement is reported (Fig. 7).

Peripheral rim enhancement on arterial phase was associated with two filling patterns: prevalently, with a rim-like centripetal pattern (75% and 60% of cases, in the literature and our experience, respectively), but not infrequently with a heterogeneous nonspecific pattern (25% and 40% of cases, respectively). The target sign was associated with a centrifugal pattern in all cases, both in the literature and in our experience.

In the literature, conventional CAs were used in 34 patients (69%), being a liver-specific CA (Gd-EOB-DTPA) adopted in 5 patients (10%); the other 10 patients (21%) received no CA or administration was unspecified. The pattern of enhancement (Table 4) was described as heterogeneous nonspecific in 51% of patients, and rim-like centripetal in 23%. Less frequently enhancement was homogeneously high in all dynamic phases (10%), or centrifugal (8%) or persistently low (8%). On arterial phase, 44% of patients showed hyperintensity (homogeneous or heterogeneous with small foci relatively less hyperintense), 35% peripheral rim enhancement, and 9% target sign aspect. On equilibrium/transitional phase, 80% of patients showed homogeneous iso- or hyperintensity, or heterogeneous hyperintensity with small foci relatively less hyperintense. On HBP, 80% of patients showed homogeneous hypointense PH lesions. Multiple PH nodules in the same liver shared a similar pattern of enhancement.

Histopathology Confirmation of PH

The diagnosis of PH for our patients was based on histopathological findings (12 core biopsies). The histological type was not specified. All 49 cases of PH in the literature had histopathological confirmation of the diagnosis as a result of either core biopsy (67%) or resection (29%) or post-mortem autopsy (4%). The histological type of PH was reported in 24 patients: 54% presented the parenchymal type, while 46%

TABLE 4. Correlation Between Enhancement Pattern and Signal Intensity on Arterial, Equilibrium/Transitional, and Hepatobiliary Phase
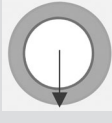
	n/N / **n/N**	Heterogeneous Nonspecific CE	Rim-Like Centripetal CE	Homogeneously High CE	Centrifugal CE	Persistently Low CE
		20/39 (51%) / **3/12 (25%)**	*9/39 (23%)* / **3/12 (25%)**	*4/39 (10%)* / **1/12 (8%)**	*3/39 (8%)* / **4/12 (34%)**	*3/39 (8%)* / **3/39 (8%)** **1/12 (8%)**
AP						
Peripheral rim	*12/34 (35%)* / **5/12 (42%)**	*3/12 (25%)* / **2/5 (40%)**	*9/12 (75%)* / **3/5 (60%)**	- / -	- / -	- / -
Heterogeneous hyperintensity	*11/34 (32%)* / **3/12 (25%)**	*11/11 (100%)* / **1/3 (34%)**	- / -	- / -	*-* / **2/3 (66%)**	- / -
Homogeneous hyperintensity	*4/34 (12%)* / **1/12 (8%)**	- / -	- / -	*4/4 (100%)* / **1/1 (100%)**	- / -	- / -
Heterogeneous hypointensity	*4/34 (12%)* / **1/12 (8%)**	*1/4 (25%)* / -	- / -	*-* / **1/1 (100%)**	- / -	*3/4 (75%)* / -
"Target" sign	*3/34 (9%)* / **2/12 (17%)**	- / -	- / -	- / -	*3/3 (100%)* / **2/2 (100%)**	- / -
EP/TP						
Peripheral rim	*1/36 (3%)* / -	*1/1 (100%)* / -	- / -	- / -	- / -	- / -
Heterogeneous hyperintensity	*12/36 (33%)* / **6/12 (50%)**	*11/12 (92%)* / **2/6 (34%)**	*-* / **1/6 (16%)**	- / -	*1/12 (8%)* / **3/6 (50%)**	- / -
Homogeneous hyperintensity	*14/36 (39%)* / **3/12 (25%)**	*4/14 (29%)* / -	*5/14 (36%)* / **2/3 (66%)**	*3/14 (21%)* / **1/3 (34%)**	*2/14 (14%)* / -	- / -
Homogenous isointensity	*3/36 (8%)* / **2/12 (17%)**	*-* / **1/2 (50%)**	*2/3 (66%)* / -	*1/3 (34)* / -	*-* / **1/2 (50%)**	- / -

TABLE 4. Continued

	n/N	Heterogeneous Nonspecific CE	Rim-Like Centripetal CE	Homogeneously High CE	Centrifugal CE	Persistently Low CE
	n/N / **n/N**	*20/39 (51%)* / **3/12 (25%)**	*9/39 (23%)* / **3/12 (25%)**	*4/39 (10%)* / **1/12 (8%)**	*3/39 (8%)* / **4/12 (34%)**	*3/39 (8%)* / **1/12 (8%)**
Homogenous hypointensity	*6/36 (17%)* / **1/12 (8%)**	*3/6 (50%)* / –	– / –	– / –	– / –	*3/6 (50%)* / **1/1 (100%)**
HBP						
Homogeneous hypointensity	*4/5 (80%)* / **5/12 (42%)**	*1/4 (25%)* / **1/5 (20%)**	*2/4 (50%)* / **1/5 (20%)**	– / –	– / **2/5 (40%)**	*1/4 (25%)* / **1/5 (20%)**
Heterogeneous hypointensity with rim/foci of relative hyperintensity	*1/5 (20%)* / **7/12 (58%)**	*1/1 (100%)* / **2/7 (29%)**	– / **2/7 (29%)**	– / **1/7 (13%)**	– / **2/7 (29%)**	– / –

The arrow in "Rim-like Centripetal CE" picture represents the progressive enhancement that spreads from the peripheral portion of the lesions toward the center. Conversely, in "Centrifugal CE" picture, the arrow indicates the gradual enhancement which originates inside the lesion and spread outwards. Literature data references: pattern of enhancement[2,3,5,10,11,17,25](3 pts),[26](9 pts),[28,29,31,32](2 pts),[33-42,44-46,48-50]; AP[3,5,10,11,25](3 pts),[26](9 pts),[28,29,31-42,44,46,48,50]; EP/TP[2,3,5,10,11,17,25](4 pts),[26](9 pts),[28,31-42,44,45,48,50]; HBP.[5,40,41,44,50]

n = total number of patients; N = number of patients; N = number of patients for whom the data are available (italic font, literature data; bold font, our experience); CE = contrast enhancement; AP = arterial phase; EP = equilibrium phase (after conventional contrast agent administration); TP = transitional phase (after liver specific contrast agent administration); HBP = hepatobiliary phase.
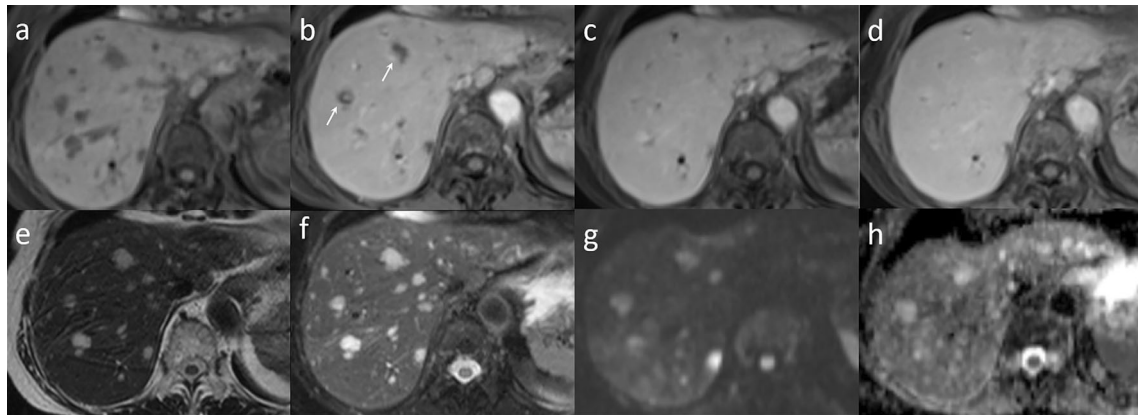
FIGURE 5: A 70-year-old female with history of biliary tract infection, recurrent abdominal pain. On MRI multiple irregularly shaped lesions are observed on both hepatic lobes. They show homogeneous signal hypointensity on unenhanced T1-weighted images (a), centrifugal pattern of enhancement from arterial (b) to portal (c) and transitional (d) phase, with target sign on arterial phase more evident in some of the nodules (b, white arrows). The homogeneous hyperintensity on T2-weighted (e) and T2-weighted fat sat images (f), and the absence of restricted diffusion on high *b*-value DWI (g) and on ADC map (h) are shown. Histological examination confirmed liver parenchyma with peliosis, characterized by dilated sinusoidal spaces with congestion.

the phlebectatic type. Histopathological finding of sinusoidal obstruction syndrome associated with PH was observed in one patient from the literature and one patient from our experience (Fig. 8).

Proposed Imaging Diagnosis

From the reports analysis, lesion characterization was proposed in 41 patients (11 out of 12 in our series and 30 out of 49 in the literature, respectively); out of these, an ultimately correct diagnosis of PH was hypothesized by MRI only in 7 cases (17%).

In case of misdiagnosis, among those believed to be malignant lesions, the most frequent ones included liver metastasis in 17 (41%) patients and hepatocellular carcinoma (HCC) in 4 (10%), while benign ones included hepatic hemangioma in 6 (15%) and inflammatory pseudotumor in 3 (7%) patients. Other less frequently proposed diagnoses are listed (Table 5).

Patient Follow-Up Examinations

Information about patient imaging or clinical follow-up exams was available for 7 (58%) patients from our experience (from 3 months to 3 years), and for 17 (35%) patients from the literature (from 3 months to 1 year). Out of these 24 patients with follow-up information, resolution or size decrease of PH nodules was reported in 7 (29%); in 4 cases (20%) such change was reported following drug cessation or therapy modification (Table 5). Numerical or size increase of PH nodules was reported in six (25%) patients, three of them receiving hormonal therapy. Finally, stable disease at 3–6 months was reported in six (25%) patients. Severe complications (eg, post-biopsy hemoperitoneum, severe liver failure, death from sepsis) arose in six (25%) patients, mostly when PH was associated with immunosuppression or severe
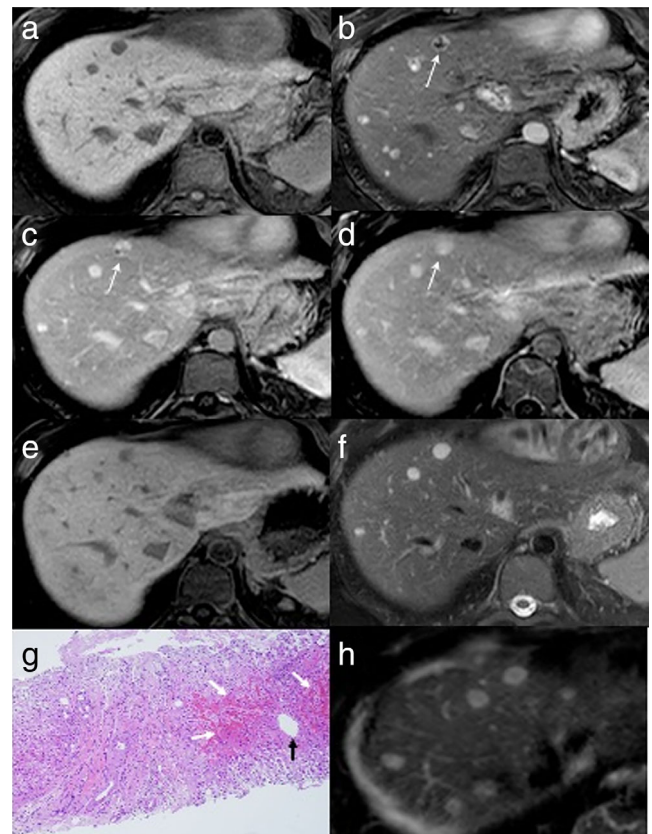
FIGURE 6: A 43-year-old male with common variable immunodeficiency. On MRI multiple hepatic round nodules appeared during immunosuppressive therapy, showing unenhanced T1 hypointensity (a), a rim-like centripetal pattern of enhancement from arterial (b) to portal (c) and transitional (d) phase (white arrow in more evident lesion), homogeneous hypointensity on hepatobiliary phase (e), homogeneous T2 hyperintensity (f). Histological examination (g, hematoxylin–eosin, original magnification ×200) shows blood filled spaces partially lined by endothelium (white arrows) around a central vein (black arrow). The findings are indicative of peliosis hepatis. Numerical and size increase of the lesion is seen on MRI at 1 year (h, T2-weighted image).

PELIOTIC PATTERNS OF ENHANCEMENT
IN RELATION WITH SITE AND EXTENSION OF SINUSOINDAL RUPTURE

FIGURE 7: Schematic representation of the most common pattern of contrast enhancement observed in peliosis hepatis. Hepa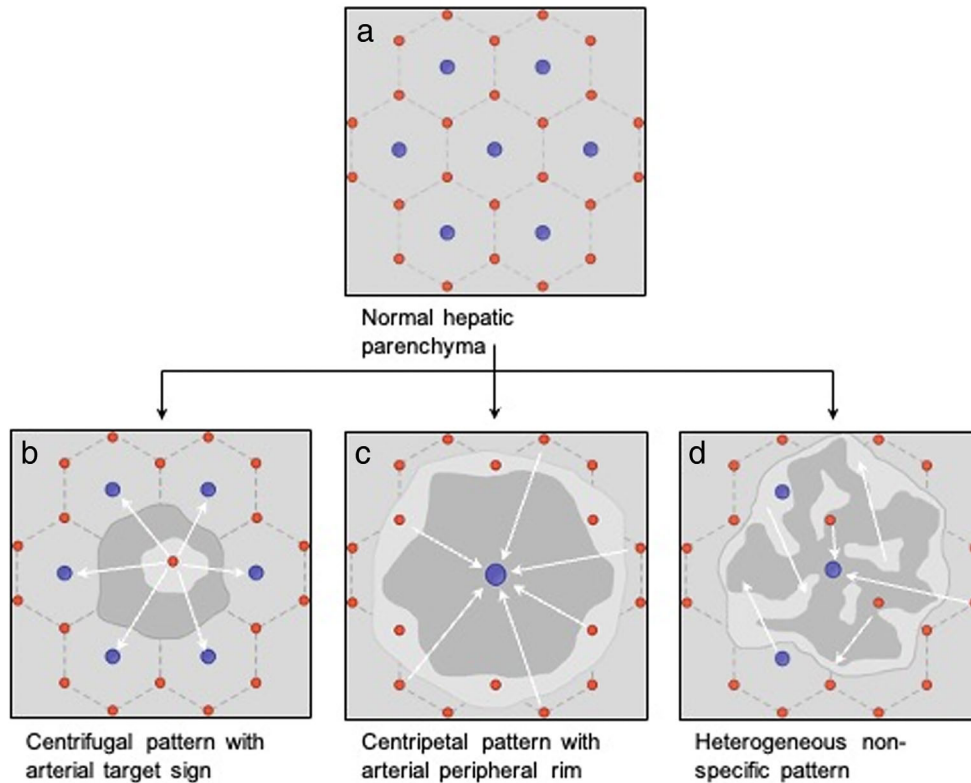tic lobule with centrilobular vein (blue circle) and arterial branch (red circle) representation in normal hepatic parenchyma is shown (a). When the endothelial damage of the sinusoids occurs around an arterial vessel, the lesion will likely show a progressive centrifugal enhancement often associated to the arterial target sign (b). If the damage is prevalently around a dilated central vein, the nodule will show an arterial peripheral rim with progressive centripetal enhancement (c). If peliotic lacunae are partly or fully thrombosed, the enhancement can be heterogeneous nonspecific (d).

hematologic disorders such as Fanconi anemia or common variable immunodeficiency (67% of cases). No associations between the pathological type of PH, patterns of enhancement, evolution during follow-up, and proposed imaging diagnosis were observed (Table 5). Given the fragmentary nature and evident variability of the data, statistical tests were not performed.

Discussion

Both our series and literature review have suggested polymorphic appearance of PH: on unenhanced imaging, a homogeneous, ill-demarcated hypo/hyperintense lesion on T1W/T2W images, without restricted diffusivity can be more frequently found. The enhancement pattern was highly variable, but more frequently it was heterogeneous nonspecific or rim-like centripetal or centrifugal, always with hypointensity on the HBP. Patients often had a history of malignancies, chronic pathologies, and drug exposure.

On imaging, PH is frequently misdiagnosed with other benign or malignant focal liver lesions.[8,9] On ultrasound (US), it can appear as a hypo- and hyperechoic lesion in patients with fatty and normal liver structure, respectively. The most common CE-US enhancement pattern is a mild heterogeneous hyper-enhancement on arterial phase, with washout in portal venous phase, similar to other hepatic tumors.[25] On computed tomography (CT), enhancement patterns are variable and PH nodules with a diameter smaller than 1 cm might be missed on unenhanced images.[2,17,27,32] Lesions can show variable echogenicity/density/SI, primarily in presence of hemorrhages or blood clots. On fluorodeoxyglucose-positron emission tomography both isometabolic and hypermetabolic PH nodules have been reported.[51,52]

Overall, no specific epidemiological or clinical features of PH have been observed. It affects adults more commonly, but it can occur at any age.[3] In line with previous work,[2,18,53] most patients in our analysis were asymptomatic at initial presentation. When present, clinical symptoms and abnormal liver tests were nonspecific. Although often idiopathic (20%–50% of cases), several conditions have been considered as possible causative factors of PH, including long-term intake of drugs, malignancies, hematological conditions, or infectious diseases.[2,18] However, currently no
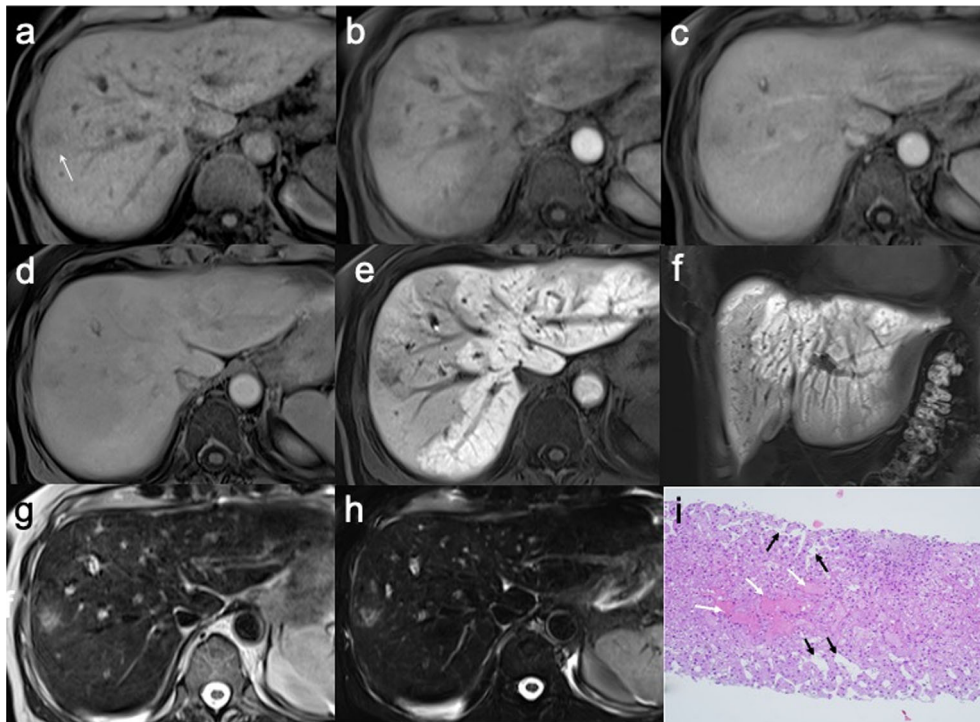
FIGURE 8: A 64-year-old female with lung cancer. MR was performed after 1 year of chemotherapy for abdominal pain. A nodule slightly hypointense on unenhanced T1-weighted image is shown (a, white arrow). On arterial (b), portal (c) and transitional (d) phase the pattern of enhancement of the lesion is heterogeneous nonspecific, while the liver parenchyma shows a mosaic pattern of enhancement, with reticular aspect on hepatobiliary phase (e, axial scan; f, coronal scan). On T2-weighted (g) and fat sat T2-weighted (h) images the nodule appears heterogeneously hyperintense. Histological examination (i, hematoxylin–eosin, original magnification ×200) shows blood filled spaces lined by endothelium (white arrows) and dilated sinusoidal spaces (black arrows).

evidence supports a direct relationship between the abovementioned factors and the development of PH.[11,54–57] Also, our analysis demonstrated that conditions associated with PH were present in most patients. Furthermore, we frequently found PH lesions to be of new onset according to imaging.

Although with some differences in rates between existing studies and our series, some reproducible and rather typical MRI features of PH might have been observed. Regarding PH nodules, those can be single or multiple, round or oval-shaped, with ill-defined or well-demarcated boundaries. A lack of mass effect on vascular/biliary structure is characteristic. Being the most frequent appearance on T1W/T2W images, a homogenous hypo/hyperintensity appearance, respectively, a higher percentage of PH nodules showed T1W and T2W heterogeneous SI in our experience vs. the literature. We believe that these differences reflect various stages and distributions of the bleeding components of the lesions or the presence of hemorrhagic necrosis.[3,32] The most part of patients showed no signs of restricted diffusivity. Targetoid appearance, with a hypointense core both on DW images and ADC map, was observed in less than one-fifth of cases. This was probably consistent with coagulative necrosis in the middle part of the lesion, showing low signal on DWI not due to high diffusivity but to an absence of diffusible substrate (spin mobile lessening effect or dark through).[58]

Differences between literature results and our series were more evident on CE-T1W images. Specifically, PH nodules mostly showed heterogeneous nonspecific enhancement in the literature vs. centrifugal enhancement in our group of patients. A similar percentage of patients showed rim-like centripetal, homogeneously high, and persistently low enhancement. On arterial phase, most patients showed hetero-/homogeneous hyperintensity or peripheral rim enhancement. The arterial target sign was less frequent, but typically always associated with a centrifugal pattern. On equilibrium/transitional phase, most patients showed hetero-/homogeneous iso/hyperintensity.

The variability in shape, edges, and enhancement of PH could be related to its pathogenesis.

Specifically, PH has often been considered a particular hepatic focal lesion, but in our opinion, it may be better understood as a type of parenchymal damage. Previous studies have suggested that the pathological mechanism behind the disease involves the loss of integrity of tissue microcirculation with the breakdown of reticulin fibers supporting hepatocytes and sinusoids.[36] Moreover, an association between PH and hepatic outflow obstruction has been reported.[11,36,44] Our analysis might confirm this association in patients with PH on chemotherapy and sinusoidal obstruction syndrome.[40] Both the two conditions would fall within the sinusoidal forms

TABLE 5. Summary of Pathological Type of Peliosis Hepatis, Associated Condition, Pattern of Enhancement, Proposed Imaging Diagnosis and Evolution During Follow-Up Examinations

	Pathology	Associated Condition	Pattern Enhancement	Proposed Diagnosis	Follow-Up
[2]	Par	Hormonal th	Heterogeneous nonspecific	PH	-
[3]	Par	-	Centrifugal	HH	
[5]	-	Hormonal th	Centripetal	adenoma	Size decrease after drug cessation
[6]	Par	Immunosuppressive th	-	Mets/primary liver malignancy/IPTL	Post biopsy hemoperitoneum, liver transplant 1 year later
[10]	Phl	Hormonal th	Centrifugal	Vascular lesion	1-year resolution
[11]	Par	-	Heterogeneous nonspecific	PH	3-month size decrease
[17]	Par	Lung cancer	Heterogeneous nonspecific	HH	
[25] 1 pt	Phl	Antineoplastic drug	Homogeneously high		
[25] 1 pt	Phl	-	Centripetal		
[26] 2 pts	-	Colorectal cancer	Heterogeneous nonspecific	Mets	
[26] 5 pts	-	Antineoplastic drug	Heterogeneous nonspecific	Mets	
[27]	Phl	Hormonal th	-		Severe liver failure
[28]	Phl	Hormonal th	Poor enhancement	HCC	Resolution after drug cessation
[29]	-	Hormonal th	Heterogeneous nonspecific	PH	Death from sepsis
[30]	-	Gastric cancer		Mets	
[31]	Par	Hormonal th	Homogeneously high	Pseudotumoral steatosis	Size increase
[32] 1 pt	Phl	Corticosteroids	Centripetal		9 weeks size decrease after drug cessation
[32] 1 pt	Par	Antineoplastic drug	Heterogeneous nonspecific		
[33]	Par	Hormonal th	Centripetal		
[34]	Phl	Antineoplastic drug	Centripetal	Mets	
[35]	Par	Bartonella infection	Heterogeneous nonspecific		
[36]	Phl	-	Heterogeneous nonspecific	Liver malignancy	
[37]	Par	Hormonal th	Centripetal		
[38]	Par	Lung cancer	Heterogeneous nonspecific	Fibrous lesion	
[39]	Phl	Hormonal th	Centrifugal	Mets/IPTL/EHE	Size increase

TABLE 5. Continued

	Pathology	Associated Condition	Pattern Enhancement	Proposed Diagnosis	Follow-Up
[40]	-	Antineoplastic drug	Poor enhancement	Mets	Size increase 3 months
[41]	-	Hepatitis C virus	Centripetal	HCC	
[42]	-	Hormonal th	Homogeneously high	Vascular lesion	Size increase
[43]	-	Biliary tract infection	-		1-year resolution
[44]	Par	-	Heterogeneous nonspecific	HCC	
[45]	-		Heterogeneous nonspecific		Post biopsy hemoperitoneum
[46]	Phl	-	Centripetal	HCC	
[47]	Par	-	-	Cystic echinococcosis	
[48]	Phl	CVI	Poor enhancement		Liver failure
[49]	-	Renal cell carcinoma	Heterogeneous nonspecific	Mets	Stable at 4 months
[50]	-	-	Centripetal	HH/Mets	Numerical and size increase
Pt 1	-	-	Centrifugal	PH	Stable at 3 years
Pt 2	-	Cocaine abuse	Centrifugal		
Pt 3	-	Biliary tract infection	Centrifugal	HH/Mets	Stable at 6 months
Pt 4	-	Hormonal th	Poor enhancement	HH/Mets	Stable at 6 months
Pt 5	-	Hormonal th	Heterogeneous nonspecific	IPTL	Stable at 3 months
Pt 6	-	Interferon th	Homogeneously high	FNH	Resolution after therapy change
Pt 7	-	Antineoplastic drug	Heterogeneous nonspecific	PH and SOS	
Pt 8	-	Hormonal th	Heterogeneous nonspecific	HH	Stable at 2 years
Pt 9	-	Hormonal th	Centripetal	Vascular lesion	
Pt 10	-	Antineoplastic drug	Centripetal	Vascular lesion	
Pt 11	-	CVI	Centripetal	PH	Numerical/size increase; death for sepsis
Pt 12	-	-	Centrifugal	PH	

[n] = corresponding reference of literature analysis; Pt(s) = patients; Pt 1 to Pt 12 = patients of our experience; Par = parenchymal type; Phl = phlebectatic type; th = therapy, CVI = common variable immunodeficiency PH = peliosis; HH = hepatic hemangioma; Mets = metastasis; IPTL = inflammatory pseudotumor of the liver; EHE = epithelioid hemangioendothelioma; HCC = hepatocellular carcinoma; FNH = focal nodular hyperplasia; SOS = sinusoidal obstruction syndrome.

of hepatic outflow obstruction, as a consequence of endothelial damage to the sinusoids, and the pattern of enhancement of the peliotic lacunae could depend on the site and extension of the sinusoidal wall rupture.[59,60] Thus, we hypothesize that if the damage is essentially located around an arterial vessel, the lesion might show a homogeneously high persisting enhancement or a progressive centrifugal enhancement with an arterial target sign. Conversely, if the damage is predominantly located around a dilated central vein, the PH nodule might show an arterial peripheral rim enhancement with progressive centripetal or heterogeneous nonspecific patterns. Lastly, if cavities are partly or fully thrombosed, or non-enhancing areas of hemorrhagic parenchymal necrosis are present, the enhancement can be heterogeneous nonspecific or persistently low. The vascular nature of peliotic lesions could be confirmed by signal hypointensity on HBP, where foci or rim of signal hyperintensity may indicate the presence of hepatocytes spared from parenchymal destruction. More specifically, the histological classification of PH into parenchymal and phlebectatic peliosis, in our opinion, appears to be outdated. In fact, classification of peliosis on the basis of absence/presence of endothelium is not tenable due to the fact that, initially, the spaces may have no endothelial lining, but re-endothelialization may occur rapidly.[61] Thus, parenchymal and phlebectatic peliosis are probably two different phases of the same process. The rupture of sinusoidal walls in the parenchymal type would constitute the early phase of PH, and the phlebectatic type would be seen as the end phase after endothelial coverage repair.[3,44,48] Furthermore, both histological types might coexist and may result in thrombosis and hemorrhage.[32] Lastly, according to previous work, we have not found distinct associations between the histological type, the pattern of enhancement, and the clinical course of the disease.[10,25,48]

With regards to the differential diagnosis, PH can be considered a great mimicker. The initial diagnostic hypothesis on MRI was different from PH in the majority of patients, consisting of 12 different types of focal liver lesions. First of all, it can be difficult to differentiate PH from metastases. The bright SI on T2W images and the longer retention of CA of PH may allow us to distinguish peliotic lesion from hypervascular metastases, which usually show rapid enhancement and frequent washout due to intratumoral neoangiogenesis.[10,17] An ill-defined margin and the lack of mass effect of PH can help in the differential diagnosis with hypovascular metastases.[10,17] In addition, peliotic lesions rarely show homogeneous signal hypointensity on ADC maps vs. metastases.[25,62]

The higher SI on T2W images and the persistent enhancement on equilibrium phase of PH may enable us to differentiate them from HCC.[25] However, HCC can show atypical enhancement patterns, intralesional complications (such as hemorrhage, cystic degeneration, and necrosis), and variable SI on HBP according to the grade of malignancy.[50,63] Lastly, not only have cases of HCC with PH in the non-cancerous parts of the liver been described, but cases of pelioid-type HCC have also been reported.[64] They are moderately or poorly differentiated HCCs, with early irregular enhancement of the peripheral part of the lesion and pooling of CA in the middle part, most likely due to extensive peliotic change.[65]

Considering benign focal liver lesions, hemangiomas are the most frequent cause of misdiagnosis. PH can show centripetal enhancement, similar to the one of typical hemangioma.[17] On the other side, atypical hemangiomas can show centrifugal enhancement.[10,17] Moreover, hemangiomas of considerable volume usually have globular (vs. rim-like of PH) peripheral progressive enhancement and a mass effect, which is not shown by PH.[8,10] Sometimes PH may show a targetoid aspect similarly to hepatic inflammatory pseudotumor. However, after CA administration, inflammatory pseudotumors most frequently show a three- or two-layered concentric targetoid aspect. In addition, they are frequently associated with the plasma positivity for IgG4.[66]

Signal hyperintensity on HBP generally enables us to differentiate between focal nodular hyperplasia and PH with homogeneously high patterns of enhancement.[67,68] It is more difficult to differentiate PH from hepatocellular adenoma, especially in case of the inflammatory type, showing high SI on T2W images, heterogeneous enhancement, and hypointensity on HBP.[69] In detail, PH-like blood-filled cavities have been observed about in 60% of these lesions, more frequently in the largest ones.[70] In these patients, biopsy is often required to reach a definitive diagnosis. According to the literature, prognosis of PH is variable. If drug-induced, it generally resolves after cessation of medications, if infection-related, it typically shows regression after appropriate treatment of the pathogen, and if idiopathic, it more often may persist.[3,17,39] In some cases, complications mainly represented by hemorrhagic events such as liver rupture and hemoperitoneum may occur.[8,71] The most severe complications arose mostly in cases where PH was associated with immunosuppression or severe hematologic disorders. This could confirm that the clinical course of PH might be determined mainly by the underlying disease that caused the peliosis, rather than by the histological type.[48]

Limitations

Regarding the literature studies, it must be emphasized that we followed the applicable PRISMA items and proposed a systematic review, but a meta-analysis was not performed. This is because the data found in the literature were very fragmented as most publications were case reports or series. So, the final analysis involved large discrepancies in the features presented, determined, in part by the great differences

regarding equipment and acquisition methods. Moreover, the very few examples and short follow-up durations of the lesions in the studies from the literature only allowed a partial evaluation of PH over time. Despite these limitations, in our opinion, the main peliosis patterns have been sufficiently described. Regarding the retrospective part of the study, a limitation was represented by a relatively small number of patients belonging to our series (nevertheless, one of the most numerous series found in the literature). A second limitation could be seen in the difference in ethnicity of cases from the existing literature, which was made up of 70% Asians, vs. our cases who were all Caucasians. Finally, we used Gd-EOB-DTPA in all of our patients. Only a few patients in the literature, conversely, were evaluated with a liver-specific CA. We are advised that by using Gd-EOB-DTPA, it is possible to experience a pseudo-wash out phenomenon due to a rapid passage of CA into the hepatocytes.[72] However, in our cases this phenomenon was never detected, probably due to the histological peculiarity of PH.

Conclusion

Our work might confirm the polymorphic appearance of PH. However, it also demonstrated that when atypical focal liver lesions with homogeneous hypo/hyperintensity on T1/T2W images, heterogeneous nonspecific or centrifugal or rim-like pattern of enhancement, hypointensity on HBP, without restricted diffusivity and a definite mass effect, the diagnosis of PH must be considered. This is particularly the case when lesions are new in onset in patients with underlying malignancies, chronic conditions, and drug exposure.

Acknowledgment

References

1. Zak FG. Peliosis hepatis. Am J Pathol 1950;26:1-15.

2. Kim SB, Kim DK, Byun SJ, et al. Peliosis hepatis presenting with massive hepatomegaly in a patient with idiopathic thrombocytopenic purpura. Clin Mol Hepatol 2015;21:387-392.

3. Crocetti D, Palmieri A, Pedullà G, Pasta V, D'Orazi V, Grazi GL. Peliosis hepatis: Personal experience and literature review. World J Gastroenterol 2015;21:13188-13194.

4. Tsokos M, Erbersdobler A. Pathology of peliosis. Forensic Sci Int 2005;149(1):25-33.

5. Hung NR, Chantrain L, Dechambre S. Peliosis hepatis revealed by biliary colic in a patient with oral contraceptive use. Acta Chir Belg 2004;104:727-729.

6. Lui WH, Chou TC, Chang SS, Hung CJ, Lin YJ, Lee PC. Peliosis hepatis in a kidney transplant recipient with manifestation as massive ascites and liver dysfunction: Case report. Transplant Proc 2014;46:630-633.

7. Yanoff M, Rawson AJ, Hepatis P. An anatomic study with demonstration of two varieties. Arch Pathol 1964;77:159-165.

8. Iannaccone R, Federle MP, Brancatelli G, et al. Peliosis hepatis: Spectrum of imaging findings. Am J Roentgenol 2006;187:43-52.

9. Dong Y, Wang WP, Lim A, et al. Ultrasound findings in peliosis hepatis. Ultrasonography 2021;40:546-554.

10. Gouya H, Vignaux O, Legmann P, de Pigneux G, Bonnin A. Peliosis hepatis: Triphasic helical CT and dynamic MRI findings. Abdom Imaging 2001;26:507-509.

11. Vignaux O, Legmann P, de Pinieux G, et al. Hemorrhagic necrosis due to peliosis hepatis: Imaging findings and pathological correlation. Eur Radiol 1999;9:454-456.

12. Wang SY, Ruggles S, Vade A, Newman BM, Borge MA. Hepatic rupture caused by peliosis hepatis. J Pediatr Surg 2001;36:1456-1459.

13. Fidelman N, LaBerge JM, Kerlan RK. SCVIR 2002 film panel case 4: Massive intraperitoneal hemorrhage caused by peliosis hepatis. J Vasc Interv Radiol 2002;13:542-545.

14. Kootte AM, Siegel AM, Koorenhof M. Generalised peliosis hepatis mimicking metastases after long-term use of oral contraceptives. Neth J Med 2015;73:41-43.

15. Kleinig P, Davies RP, Maddern G, Kew J. Peliosis hepatis: Central "fast surge" ultrasound enhancement and multislice CT appearances. Clin Radiol 2003;58:995-998.

16. Savastano S, San Bortolo O, Velo E, Rettore C, Altavilla G. Pseudotumoral appearance of peliosis hepatis. Am J Roentgenol 2005;185:558-559.

17. Steinke K, Terracciano L, Wiesner W. Unusual cross-sectional imaging findings in hepatic peliosis. Eur Radiol 2003;13:1916-1919.

18. Elsayes KM, Shaaban AM, Rothan SM, et al. A comprehensive approach to hepatic vascular disease. Radiographics 2017;37:813-836.

19. Hui CL, Lee ZJ. Hepatic disorders associated with exogenous sex steroids: MR imaging findings. Abdom Radiol 2019;44:2436-2447.

20. McInnes MDF, Moher D, Thombs BD, et al. Preferred reporting items for a systematic review and meta-analysis of diagnostic test accuracy studies: The PRISMA-DTA statement. JAMA 2018;319:388-396.

21. Couinaud C. The parabiliary venous system. Surg Radiol Anat 1998;10:311-316.

22. Schardt C, Adams MB, Owens T, Keitz S, Fontelo P. Utilization of the PICO framework to improve searching PubMed for clinical questions. BMC Med Inform Decis Mak 2007;7:16.

23. Moola S, Munn Z, Tufanaru C, et al. Chapter 7: Systematic reviews of etiology and risk. In: Aromataris E, Munn Z, editors. *JBI manual for evidence synthesis*: JBI; 2020. https://doi.org/10.46658/JBIMES-20-08

24. Munn Z, Barker TH, Moola S, et al. Methodological quality of case series studies: An introduction to the JBI critical appraisal tool. JBI Evid Synth 2020;18(10):2127-2133. https://doi.org/10.11124/JBISRIR-D-19-00099.

25. Kim SH, Lee JM, Kim WH, Han JK, Lee JY, Choi BI. Focal peliosis hepatis as a mimicker of hepatic tumors: Radiological-pathological correlation. J Comput Assist Tomogr 2007;31:79-85.

26. Zhu K, Wang W, Luo R, et al. Newly detected liver nodules with a history of colorectal cancer: Are they metastatic? Review of 2,632 cases in a single center. Ann Transl Med 2021;9:1079.

27. Toyoda S, Takeda K, Nakagawa T, Matsuda A. Magnetic resonance imaging of peliosis hepatis: A case report. Eur J Radiol 1993;16:207-208.

28. Maves CK, Caron KH, Bisset GS 3rd, Agarwal R. Splenic and hepatic peliosis: MR findings. AJR Am J Roentgenol 1992;158:75-76.

29. Saatci I, Coskun M, Boyvat F, Cila A, Gürgey A. MR findings in peliosis hepatis. Pediatr Radiol 1995;25:31-33.

30. Tateishi T, Machi J, Morioka WK. Focal peliosis hepatis resembling metastatic liver tumor. J Ultrasound Med 1998;17:581-584.

31. Ferrozzi F, Tognini G, Zuccoli G, Cademartiri F, Pavone P. Peliosis hepatis with pseudotumoral and hemorrhagic evolution: CT and MR findings. Abdom Imaging 2001;26:197-199.

32. Verswijvel G, Janssens F, Colla P, et al. Peliosis hepatis presenting as a multifocal hepatic pseudotumor: MR findings in two cases. Eur Radiol 2003;13:L40-L44.

33. Yekeler E, Dursun M, Tunaci A, Cevikbas U, Rozanes I. Diagnosing of peliosis hepatis by magnetic resonance imaging. J Hepatol 2004; 41:351.

34. Xiong WJ, Hu LJ, Jian YC, et al. Focal peliosis hepatis in a colon cancer patient resembling metastatic liver tumor. World J Gastroenterol 2012; 18:5999-6002.

35. Pan W, Hong HJ, Chen YL, Han SH, Zheng CY. Surgical treatment of a patient with peliosis hepatis: A case report. World J Gastroenterol 2013;19:2578-2582.

36. Huang CY, Wang ZW. Peliosis hepatis mimicking hepatic malignancy: A case report. J Dig Dis 2013;14:272-275.

37. Grønlykke L, Tarp B, Dutoit SH, Wilkens R. Peliosis hepatis: A complicating finding in a case of biliary colic. BMJ Case Rep 2013;2013: bcr2013200539.

38. Ben Hassen W, Wagner M, Lucidarme O. Unusual hepatic lesion in a patient with a lung tumor. Gastroenterology 2014;147:e7-e8.

39. Hidaka H, Ohbu M, Nakazawa T, Matsumoto T, Shibuya A, Koizumi W. Peliosis hepatis disseminated rapidly throughout the liver in a patient with prostate cancer: A case report. J Med Case Reports 2015;9:194.

40. Choi JH, Won YW, Kim HS, Oh YH, Lim S, Kim HJ. Oxaliplatin-induced sinusoidal obstruction syndrome mimicking metastatic colon cancer in the liver. Oncol Lett 2016;11:2861-2864.

41. Lai WJ, Chiu NC, Chau GY. Hepatobiliary and pancreatic: Focal peliosis hepatis mimicking hepatocellular carcinoma in a hepatitis B carrier. J Gastroenterol Hepatol 2016;31:1073.

42. Zucchetti BM, Shimada A, Siqueira LT. Peliosis hepatis simulates liver metastases. J Glob Oncol 2018;4:1-3.

43. Dai YN, Ren ZZ, Song WY, et al. Peliosis hepatis: 2 case reports of a rare liver disorder and its differential diagnosis. Medicine (Baltimore) 2017;96:e6471.

44. Tan CHN, Soon GST, Kow WCA. Liver lesions detected in a hepatitis B core total antibody-positive patient masquerading as hepatocellular carcinoma: A rare case of peliosis hepatis and a review of the literature. Ann Hepatobiliary Pancreat Surg 2017;21:157-162.

45. Biswas S, Gogna S, Patel P. A fatal case of intra-abdominal hemorrhage following diagnostic blind percutaneous liver biopsy in a patient with peliosis hepatis. Gastroenterology Res 2017;10:318-321.

46. Chen CY, Wang YP, Lu CL. An unusual hepatic mass in a young man. Gastroenterology 2019;157:e4-e5.

47. Liu J, Wang Y, Yin S, Ke N, Liu X. Huge peliosis hepatis mimicking cystic echinococcosis: A case report. Medicine (Baltimore) 2019;98: e18141.

48. Angulo E, Joyner S, Majeed NK, Nyenhuis S. A rare case of peliosis hepatis in primary immune deficiency. SAGE Open Med Case Rep 2020;17(8):2050313X20931996.

49. Maruyama H, Takahashi K, Ishikawa N, et al. A rare case of peliosis hepatis in a patient with chronic renal failure and renal cell carcinoma. Clin J Gastroenterol 2020;13:403-407.

50. Yoshida M, Utsunomiya D, Takada S, et al. The imaging findings of peliosis hepatis on gadoxetic acid enhanced MRI. Radiol Case Rep 2020;15:1261-1265.

51. Levin D, Hod N, Anconina R, Ezroh Kazap D, Shaco-Levy R, Lantsberg S. Peliosis hepatis simulating metastatic liver disease on FDG PET/CT. Clin Nucl Med 2018;43:e234-e236.

52. Seo M, Lee SH, Han S, Sung C, Son DH, Lee JJ. Peliosis hepatis shows isometabolism on (18)F-FDG PET/CT: Two case reports. Nucl Med Mol Imaging 2014;48:309-312.

53. Cimbanassi S, Aseni P, Mariani A, Sammartano F, Bonacina E, Chiara O. Spontaneous hepatic rupture during pregnancy in a patient with peliosis hepatis. Ann Hepatol 2015;14:553-558.

54. Downes RO, Cambridge CL, Diggiss C, Iferenta J, Sharma M. A case of intra-abdominal hemorrhage secondary to peliosis hepatis. Int J Surg Case Rep 2015;7C:47-50.

55. Radin DR, Kanel GC. Peliosis hepatis in a patient with human immunodeficiency virus infection. Am J Roentgenol 1991;156:91-92.

56. Usatin MS, Wigger HJ. Peliosis hepatis in a child. Arch Pathol Lab Med 1976;100:419-421.

57. Degott C, Rueff B, Kreis H, Duboust A, Potet F, Benhamou JP. Peliosis hepatis in recipients of renal transplants. Gut 1978;19:748-753.

58. Colagrande S, Belli G, Politi LS, Mannelli L, Pasquinelli F, Villari N. The influence of diffusion- and relaxation-related factors on signal intensity: An introductive guide to magnetic resonance diffusion-weighted imaging studies. J Comput Assist Tomogr 2008;32:463-474.

59. You SH, Park BJ, Kim YH. Hepatic lesions that mimic metastasis on radiological imaging during chemotherapy for gastrointestinal malignancy: Recent updates. Korean J Radiol 2017;18:413-426.

60. Calistri L, Rastrelli V, Nardi C, et al. Imaging of the chemotherapy-induced hepatic damage: Yellow liver, blue liver, and pseudocirrhosis. World J Gastroenterol 2021;27:7866-7893.

61. Zafrani ES. An additional argument for a toxic mechanism of peliosis hepatis in man. Hepatology 1990;11:322-323.

62. Colagrande S, Castellani A, Nardi C, Lorini C, Calistri L, Filippone A. The role of diffusion-weighted imaging in the detection of hepatic metastases from colorectal cancer: A comparison with unenhanced and Gd-EOB-DTPA enhanced MRI. Eur J Radiol 2016;85:1027-1034.

63. Kovac JD, Milovanovic T, Dugalic V, Dumic I. Pearls and pitfalls in magnetic resonance imaging of hepatocellular carcinoma. World J Gastroenterol 2020;26:2012-2029.

64. Hoshimoto S, Morise Z, Suzuki K, et al. Hepatocellular carcinoma with extensive peliotic change. J Hepatobiliary Pancreat Surg 2009;16: 566-570.

65. Nomura Y, Nakashima O, Kumabe T, et al. Clinicopathologic analysis of the simple nodular type of well-differentiated hepatocellular carcinoma with extensive peliotic change. J Gastroenterol Hepatol 2014;29: 1494-1499.

66. Calistri L, Maraghelli D, Nardi C, et al. Magnetic resonance imaging of inflammatory pseudotumor of the liver: A 2021 systematic literature update and series presentation. Abdom Radiol 2022;47:2795-2810.

67. Asbach P, Klessen C, Koch M, Hamm B, Taupitz M. Magnetic resonance imaging findings of atypical focal nodular hyperplasia of the liver. Clin Imaging 2007;31:244-252.

68. Fujiwara H, Sekine S, Onaya H, Shimada K, Mikata R, Arai Y. Ring-like enhancement of focal nodular hyperplasia with hepatobiliary-phase Gd-EOB-DTPA-enhanced magnetic resonance imaging: Radiological-pathological correlation. Jpn J Radiol 2011;29:739-743.

69. Grazioli L, Olivetti L, Mazza G, Bondioni MP. MR imaging of hepatocellular adenomas and differential diagnosis dilemma. Int J Hepatol 2013; 2013:374170.

70. Paradis V, Champault A, Ronot M. Telangiectatic adenoma: An entity associated with increased body mass index and inflammation. Hepatology 2007;46:140-146.

71. Charatcharoenwitthaya P, Tanwandee T. Hepatobiliary and pancreatic: Spontaneous intrahepatic hemorrhage from peliosis hepatis—An uncommon complication of a rare liver disorder. J Gastroenterol Hepatol 2014;29:1754.

72. Pradella S, Lucarini S, Colagrande S. Liver lesion characterization: The wrong choice of contrast agent can mislead the diagnosis of hemangioma. AJR Am J Roentgenol 2012;199:W662.